Physica A 490 (2018) 331–337

Contents lists available at ScienceDirect

Physica A

journal homepage: www.elsevier.com/locate/physa

Structure and dynamics of water inside hydrophobic and hydrophilic nanotubes

Mateus Henrique Köhler [a,*], José Rafael Bordin [b], Leandro B. da Silva [c], Marcia C. Barbosa [a]

[a] Instituto de Física, Universidade Federal do Rio Grande do Sul, Caixa Postal 15051, 91501-970, Porto Alegre, Brazil
[b] Campus Caçapava do Sul, Universidade Federal do Pampa, 96570-000, Caçapava do Sul, Brazil
[c] Departamento de Física, Universidade Federal de Santa Maria, Santa Maria, Brazil

HIGHLIGHTS

- Water structure and dynamics are strongly influenced by polarity.
- The influence is negligible for wider nanotubes.
- At low density, water present smaller diffusion than at higher densities.

ARTICLE INFO

Article history:
Received 25 April 2017
Available online 1 September 2017

Keywords:
Confined water
Water diffusion
Hydrophobicity
Hydrophilicity

ABSTRACT

We have used Molecular Dynamics simulations to investigate the structure and dynamics of TIP4P/2005 water confined inside nanotubes. The nanotubes have distinct sizes and were built with hydrophilic or hydrophobic sites, and we compare the water behavior inside each nanotube. Our results shows that the structure and dynamics are strongly influenced by polarity inside narrow nanotubes, where water layers were observed, and the influence is negligible for wider nanotubes, where the water has a bulk-like density profile. As well, we show that water at low density can have a smaller diffusion inside nanotubes than water at higher densities. This result is a consequence of water diffusion anomaly.

1. Introduction

Since its discovery [1], carbon nanotubes (CNTs) has emerged as promising model systems for nanoconfinement studies of fluids. In this respect, it has been used in a wide range of applications such as water filtration [2], single-molecule sensors [3], ion selectivity [4], and energy conversion and storage [5]. In the case of nanoconfined water solutions the efficiency of the system is determined by the water–CNT interaction. This assumption can be tested by applying electric fields [6], decorating CNT walls [7], adding surfactants [8] and many others synthetization procedures.

Although not expected, the hydrophobic inner of a pristine CNT allows the water molecules not just to enter the nanotube cavity [9] but also to present a flow rate that exceeds by three orders of magnitude the values predicted by the continuum hydrodynamics theory [10,11]. Tuning the water–CNT interaction, by making it more hydrophilic or hydrophobic, is important either to achieve higher water permeation or to induce it to experience structural and dynamical transitions [12]. However, the impact of hydrophobicity over water structure and dynamics is also under debate and may lead to significant

* Corresponding author.
E-mail address: mateus.kohler@ufrgs.br (M.H. Köhler).

http://dx.doi.org/10.1016/j.physa.2017.08.030
0378-4371/

changes in its behavior [13–15]. The synthesis of chemically functionalized nanotubes with hydrophobic and hydrophilic sites [16], as in biological channels [17], adds even more complexity to this picture and presents an opportunity to study the effect of polarity heterogeneity over confined water properties.

By providing site-specific details of water properties, molecular dynamics (MD) simulations has been proved useful in the study of local structuration and quantification of water flux inside heterogeneous nanotubes [18–21]. Moskowitz and colleagues [22] has found that both the occupancy and the water flux are more sensitive to the fraction of hydrophilic atoms than to its arrangement. However, when located in the tube entrance, the hydrophobic atoms can play some role, lowering the filling rate [19]. Recently, by tuning the strength of water–nanotube attractions, Xu and his group [18] has found a maximal flow when empty states are present in the inner of the nanotube, which is unexpected since in this situation the wired hydrogen-bonding network (prerequisite for high water permeability) is broken.

In the present study we use MD simulations to examine the impact of nanotube polarity over the mobility and structure of the confined water molecules at different density regimes. Hydrophobic and hydrophilic atoms were distributed in a honeycomb lattice to form the model tubular nanochannel. The size effect is also evaluated by varying the nanotube diameter. The paper is organized as follows. In Section 2, the computational details and the methods are described, in Section 3 the main results of the dynamic and structural properties of the confined water are discussed. Conclusions are presented in Section 4.

2. Methods

2.1. Water and nanotube models

Molecular dynamics were performed using the LAMMPS package [23] for simulations of TIP4P/2005 water [24] confined inside nanotubes. The nanotube atoms are arranged on a honeycomb lattice. Two different atom types were used to build the nanotube. These two atom types differ only by their Lennard-Jones (LJ) parameters of interaction with water, and correspond to sp^2-hybridized carbon with $\varepsilon_{CO} = 0.478$ kJ/mol and $\sigma_{CO} = 0.328$ nm (labeled hydrophilic due to water attractive character) and reduced carbon–water interaction strength with $\varepsilon_{CO} = 0.27$ kJ/mol and $\sigma_{CO} = 0.341$ (namely hydrophobic), as done in previous works [12,22]. We considered (n, n) nanotubes, with $n = 10$, 16 and 30. The choice of TIP4P/2005 over many other models available in the literature was due to its accuracy in calculating transport properties of water at ambient conditions [24,25]. Particularly for the diffusion coefficient, we have found 2.32×10^9 m^2/s, which is in close agreement to previous theoretical [26] and experimental works [27].

Periodic boundary conditions were applied to simulate isolated infinite nanotubes. Cutoff distances for LJ and Coulomb interactions are 1.0 and 1.2 nm, respectively. Long-range Coulomb interactions was handled using particle–particle particle–mesh method [28]. The simulations were conducted in the NVT ensemble at temperature 300 K fixed by a Nosé-Hoover thermostat [29,30]. The system was equilibrated with a 15 ns simulation, followed by 15 ns of data accumulation. The timestep is 1 fs. In all simulations the geometry of water molecules was constrained by the SHAKE algorithm [31].

2.2. Simulational details

The water radial density profile was evaluated by dividing the inner of the nanotube in concentric cylindrical shells and averaging the number of oxygen atoms in each shell along the simulation.

The diffusion mechanism of a fluid can be reflected by the scaling behavior between the mean squared displacement (MSD) and time [32]:

$$\left\langle \left|\vec{r}(t) - \vec{r}(0)\right|^2 \right\rangle \propto Dt^{\alpha} \tag{1}$$

where $\left\langle \left|\vec{r}(t) - \vec{r}(0)\right|^2 \right\rangle$ is referred as the MSD, $\langle\rangle$ denotes an average over all the molecules and $\vec{r}\,(t)$ is the displacement of a molecule during the time interval t. The α exponent refers to the diffusion regime: $\alpha = 1$ for the linear Fickian diffusion, $\alpha > 1$ for superdiffusive and $\alpha < 1$ for subdiffusive regime. In the bulk phase, the water molecules diffuse as the Fickian type while for the water confined in CNTs, the diffusion behavior becomes extraordinary due to the nanoscale confinement [20,33].

For a fluid, the statistical error could be reduced by averaging over all the MSD components. But the nanopore confinement in the x and y directions hinders the radial displacement of the molecules. Therefore, The radial MSD is almost zero for all cases studied here and only the axial MSD will be considered.

We use the effective diameter [34]

$$d_{eff} = d - \sigma_{\mathrm{CO}},$$

where d is the nominal diameter and σ_{CO} is the Lennard-Jones (LJ) parameter for carbon–oxygen interaction. to calculate the water density inside the nanotube. In terms of d_{eff}, the effective density is then given by

$$\rho_{eff} = \frac{M}{\pi \cdot \ell \cdot \left(\frac{\mathrm{d}_{eff}}{2}\right)^2}, \tag{2}$$

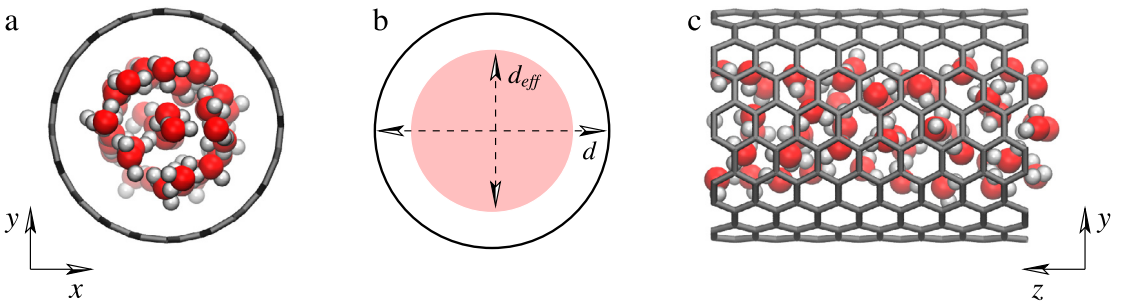

Fig. 1. (a) (10,10) nanotube filled with water and (b) definition of d_{eff} and d. In (c) we can see a side view of the nanotube.

Table 1
Nominal diameter d, length ℓ, number of enclosed molecules N and the range of *effective densities* (ρ_{eff}) for the nanotube samples.

Chirality	d (nm)	ℓ (nm)	N	ρ_{eff} (g/cm^{-3})
0.92(10,10)	1.35	37.14	540–1260	0.53–1.25
0.92(16,16)	2.17	11.07	550–1275	0.55–1.30
0.92(30,30)	4.07	8.85	1870–4360	0.57–1.35

where M is the total water mass into the pore and ℓ is the nanotube length. In Fig. 1(b) we represent the nominal and effective diameters of nanotube samples.

Based on our previous work [34], we have chosen three representative effective densities for the selected nanotubes. In Table 1 the nanotube chirality, nominal diameter d, length ℓ, number of enclosed water molecules N and the considered effective densities ρ_{eff} are presented.

3. Results and discussion

3.1. Water structure

Water structure and dynamics under hydrophobic and hydrophilic confinement is relevant to understand and develop new technologies, as well to understand aspects of life and basic science. In proteins, non-polar cavities are often located at the active site and are thought to be involved in the uptake, transfer, and release of both non-polar and polar molecules [35]. Markedly, non-polar or weakly polar pores play a prominent role in aquaporin water channels [36]. In such systems, water occupies their weakly polar pores at least transiently, exhibiting anomalous diffusion and dipoles aligned with the transmembrane axis. The pore polarity is therefore an important ingredient in the confined water properties.

In order to understand the behavior of water confined in hydrophobic and hydrophilic nanotubes at different densities, we first discuss the water molecules arrangement inside these structures. For the lower densities, $\rho_{eff} \sim 0.5$ g/cm^3, water organizes in semi-filled states with formation of bubble-like structures in hydrophilic and hydrophobic pores, as can be seen in Fig. 2. Here, we can see that the bubble inside hydrophilic nanopore is more compact than in the hydrophobic case. This indicates that the wall–water interaction affects the molecules structure in the axial direction. Hummer and co-workers [12] have highlighted the existence of sharp, two-state transitions between empty and filled states of water in such rigid hydrophobic structures. In fact, the density of water inside nanopores can be tuned by electric fields [37,38], applied pressure [39] or even functionalization [40].

This arrangement makes the water molecules more susceptible to the wall hydrophilicity, since the water–water interactions are weakened. It becomes clear in Fig. 3, where we show the density radial distribution profile for the three different nanopore radii.

Fig. 3(a), (b) and (c) reveals that, for the lower densities and all nanopore radii, the water inside the hydrophilic pore is more structured than inside the hydrophobic nanotube. For all nanotube radii, in the hydrophilic confinement the water molecules are strongly attracted to the water–wall interface, presenting a dense packing arrangement. This is not so evident for the hydrophobic confinement, where the water molecules present a more distributed density profile. For the narrowest (10,10) nanopore the water forms a concentric layer near the wall with a single line of molecules in the center. As the radius increases for the (16,16) and (30,30) nanotubes the water shows two concentric layer near the nanotube wall and a bulk-like profile in the nanotube center for hydrophilic nanopores, and only one concentric layer near the wall for the hydrophobic case. This indicates that, for low densities, the water structure inside chemically functionalized nanotubes is distinct from the observed for carbon nanotubes.

Increasing the density, at density ~ 0.9 g/cm^3, the radial density distribution, shown in Fig. 3(d), (e) and (f), indicates that the water molecules are more packed in the hydrophilic wall than in the hydrophobic. However, the number of layers is now

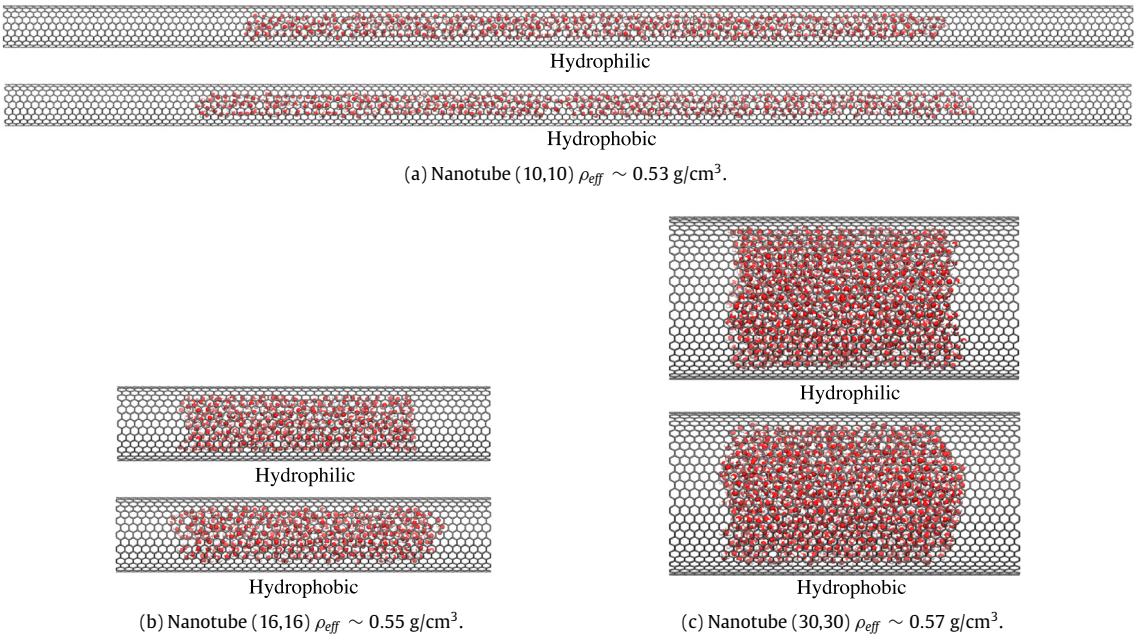

(a) Nanotube (10,10) $\rho_{eff} \sim 0.53$ g/cm^3.

(b) Nanotube (16,16) $\rho_{eff} \sim 0.55$ g/cm^3.

(c) Nanotube (30,30) $\rho_{eff} \sim 0.57$ g/cm^3.

Fig. 2. Snapshot of the lowest ρ_{eff} for both hydrophilic and hydrophobic (a) (10,10), (b) (16,16) and (c) (30,30) nanotube.

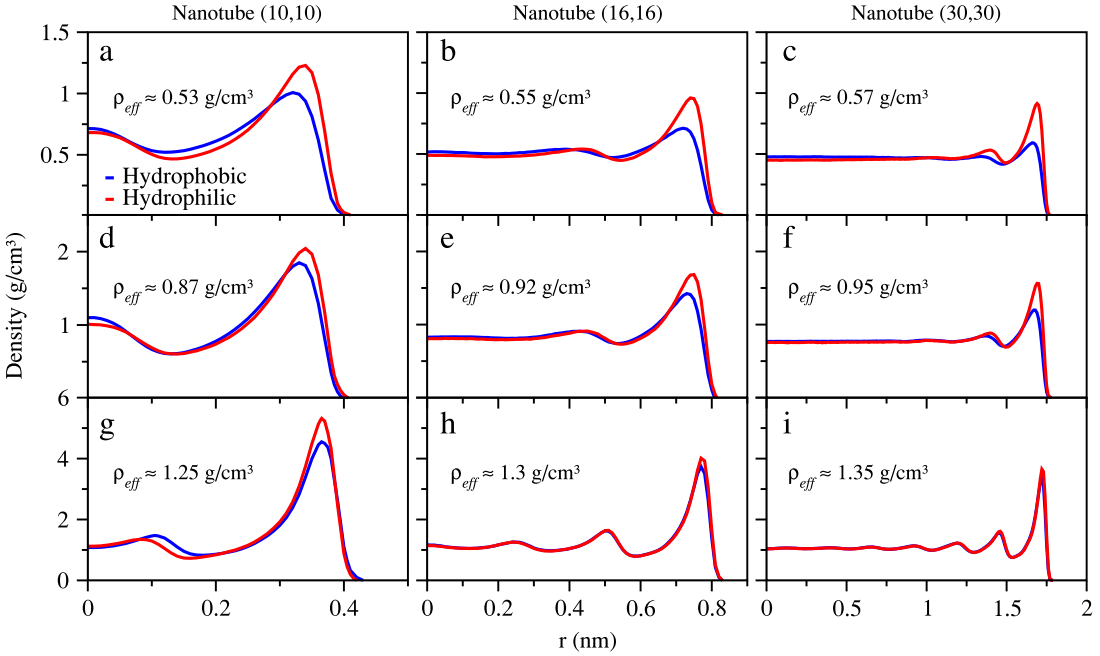

Fig. 3. Radial density distribution of oxygen atoms inside: (a) (10,10), (b)(16,16) and (c) (30,30) nanotubes, where r = 0 is at the center of the tube.

the same in all the cases. Inside (10,10) nanotubes, the water is structured in a concentric layer near the wall with a single line of molecules in the center. For (16,16) and (30,30) nanotubes the water have two concentric layers near the wall and a bulk-like profile in the center. However, the second layer for hydrophobic confinement is slightly shifted to the center of the nanotube. Therefore, for densities ~ 0.9 g/cm^3 the water–wall interaction affects the contact and the second layer, leading to a higher packing for hydrophilic nanopores, in agreement with first principle computational studies [41].

When the density is ~ 1.3 g/cm^3 we only observe a significant difference in the water structure for the (10,10) nanotube, Fig. 3(g). In this case, the central layer is strongly affected. For hydrophobic nanopores it is more close to the wall than

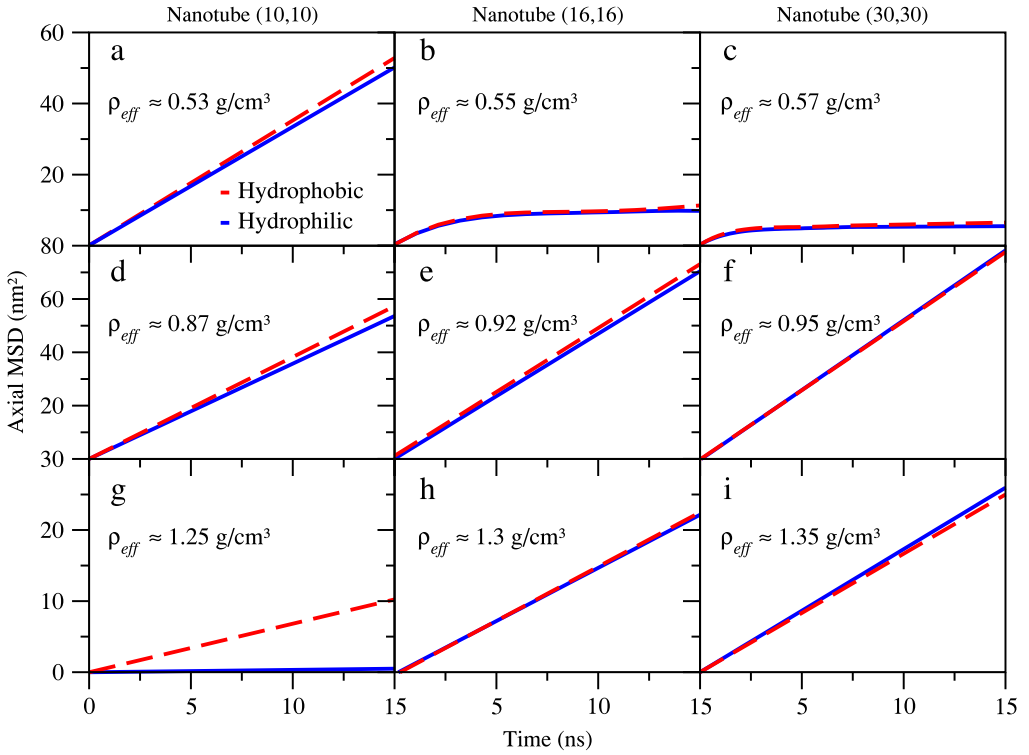

Fig. 4. Time evolution of the mean squared displacement of water oxygen atoms for some selected effective densities. The solid line stands for hydrophilic water–nanotube interaction and the dashed line for the hydrophobic interaction.

for the hydrophilic case. Inside wider nanopores, shown in Fig. 3(h) and (i), only the contact layer has a small difference, and a layered structure was obtained—4 layers inside (16,16) nanotubes and 5 concentric layers with a central bulk-like fluid for (30,30) nanotubes. This shows that at high densities the wall–water interaction is overcome by the water–water interaction. These results are relevant for biological channels and chemically modified nanotubes with polar and apolar sites, since it shows that the water structure near these sites will be affected not only by the water–wall interaction, but the water density inside the channel also plays a major role.

3.2. Water diffusion

Fluids structure and diffusion inside nanopores are strongly related [42–45]. Therefore, distinct structural regimes can lead to different diffusive behaviors. In Fig. 4, we present the axial MSD curves for water at selected densities filling (10,10), (16,16) and (30,30) nanotubes. Particularly, the diffusive regime can be defined by the scaling factor between the MSD and the exponent of time, t^{α}. For regular, or Fick, diffusive process, $\alpha = 1.0$. If $\alpha > 1.0$ we say that the system is superdiffusive, and if $\alpha < 1.0$ the regime is subdiffusive.

When $\rho_{eff} \sim 0.5$ g/cm^3, we can see that inside (10,10) nanotubes, Fig. 4(a), water diffuses faster inside hydrophobic pores than in hydrophilic pores. As well, a Fick regime is observed. Analyzing the density in Fig. 3(a), we can see that water is more packed to the hydrophilic wall. Thereafter, the friction between water and nanopore is higher, slowing the diffusion. Increasing the nanopore radius, Fig. 4(b) and (c), a distinct diffusive regime is observed. The systems shows an anomalous, subdiffusive regime. In these cases, the axial MSD is not linear and reaches a plateau at about 3 ns.

To understand this plateau, we plot in Fig. 5 the axial density profile for hydrophilic (16,16) nanotubes with densities $\rho_{eff} = 0.55$ g/cm^3 (solid red line) and $\rho_{eff} = 0.92$ g/cm^3 (solid black line). Once the densities are different, we plot the normalized density,

$$\rho_{\text{norm}}(z) = \frac{\rho_{eff}(z)}{\int \rho(z)dz} .$$

As Fig. 5 shows, the water have distinct profiles for each density. For $\rho_{eff} = 0.92$ g/cm^3 the water molecules are uniformly distributed in the z-direction. However, for the lower density there is a region of higher concentration of the particles. This indicates that the bubble shown in Fig. 2 remain more time in a specific region of the nanotube. Therefore, after a initial diffusion, that we can see in the MSD Fig. 4(b), the bubble stops her movement in the z-direction, leading to the plateau in

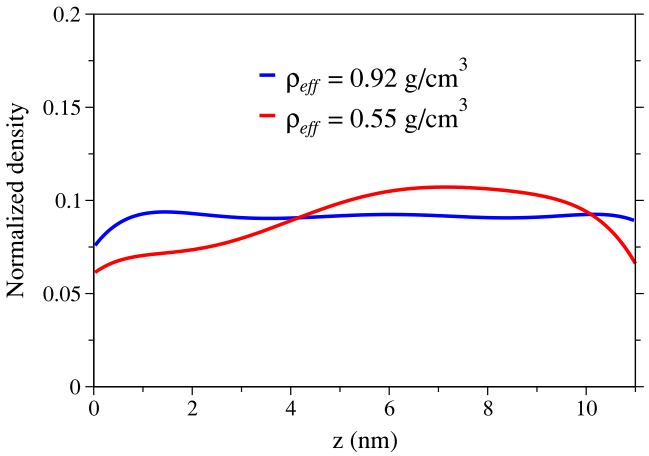

Fig. 5. Normalized axial density distribution of oxygen atoms inside hydrophilic (16,16) nanotubes with densities $\rho_{eff} \sim 0.5$ g/cm^3 (solid red line) and $\rho_{eff} \sim 0.9$ g/cm^3 (solid black line).

the MSD. To ensure that this plateau was not a equilibration problem, we run simulations up to 30 ns, and essentially the same MSD was obtained.

At the intermediate density $\rho_{eff} \sim 0.9$ g/cm^3 a Fick diffusive regime was obtained for all nanotube radii, as we show in Fig. 4(d), (e) and (f). Inside (10,10) and (16,16) nanotubes the diffusion is higher for hydrophobic confinement. Again, this is result of the higher friction with the hydrophilic wall. However, for (30,30) nanotubes there is no noticeable difference in the MSD for hydrophilic and hydrophobic nanopores. Basically, the bulk-like region, observed in Fig. 3(f), dominates the dynamical behavior, and the wall effects are less significant than for narrow nanotubes.

For the highest density, $\rho_{eff} \sim 1.3$ g/cm^3, and the narrower nanopores, the distinct water–wall interactions leads to completely different diffusive regimes. Inside hydrophobic (10,10) nanotubes the water diffuses in a Fick regime, as we shown in Fig. 4(g). This was observed in previous works for hydrophobic confinement [20,46]. Nevertheless, inside hydrophilic nanotube the system is in a solid-like state, with no diffusion. Finally, inside (16,16) and (30,30) nanotubes the diffusive behavior is the same. This was expected once the structural behavior was also the same.

Inside narrow (10,10) nanotube, either hydrophobic or hydrophilic, the number of first water neighbors is lower, and consequently the number of hydrogen bonds [47]. This leads to suppressing the strength of water–water attraction over the water–carbon interactions. In such case, the polarity of the nanotube wall plays an important role on the water mobility, rather than in larger (16,16) and (30,30) nanotubes.

4. Conclusions

We have analyzed the structural and dynamical behavior of water inside hydrophobic and hydrophilic nanotubes with distinct radii. Our results shows that both structure and diffusion are affected by the wall–water interaction. However, this influence is different accordingly with the water density inside the nanopore. As well, we have showed the strong relation between confined water structure and dynamics. The water packing at the nanopore wall affects the MSD inside the narrowest nanopores, specially for the lower densities. For wider (30,30) nanopores, our results shows that the water–wall interaction is less relevant once the fluid structure is bulk-like.

These findings shades some light on nanofluidics, and are helpful to understand the distinct behavior of water near polar or apolar sites in biological transmembrane channels, biomolecules hydration dynamics and chemically functionalized carbon, boron-nitrate or carbon doped boron-nitride nanotubes.

Acknowledgments

The authors acknowledge Brazilian science agencies CAPES and CNPq for financial support.

References

[1] S. Iijima, Helical microtubules of graphitic carbon, Nature 354 (1991) 56–58.
[2] B. Lee, Y. Baek, M. Lee, D.H. Jeong, H.H. Lee, J. Yoon, Y.H. Kim, A carbon nanotube wall membrane for water treatment, Nature Comm. 6 (2015) 7109.
[3] J. Geng, K. Kim, J. Zhang, A. Escalada, R. Tunuguntla, L.R. Comolli, F.I. Allen, A.V. Shnyrova, K. Cho, D. Munoz, Y.M. Wang, C.P. Grigoropoulos, C.M. Ajo-Franklin, V.A. Frolov, A. Noy, Stochastic transport through carbon nanotubes in lipid bilayers and live cell membranes, Nature 514 (2014) 612–615.
[4] M. Thomas, B. Corry, T.A. Hilder, Small 10 (2014) 1453–1465.
[5] H.G. Park, Y. Jung, Carbon nanofluidics of rapid water transport for energy applications, Chem. Soc. Rev. 43 (2014) 565–576.

[6] J. Shin, G. Kim, I. Kim, H. Jeon, T. An, G. Lim, Ionic liquid flow along the carbon nanotube with dc electric field, Sci. Rep. 5 (2015) 11799.
[7] A. Siddiqa, A. Shahid, R. Gill, Silica decorated CNTs sponge for selective removal of toxic contaminants and oil spills from water, J. Env. Chem. Eng. 3 (2) (2015) 892–897.
[8] C.-J. Shih, S. Lin, M.S. Strano, D. Blankschtein, Understanding the stabilization of single-walled carbon nanotubes and graphene in ionic surfactant aqueous solutions: large-scale coarse-grained molecular dynamics simulation-assisted DLVO theory, J. Phys. Chem. C 119 (2) (2015) 1047–1060.
[9] N. Naguib, H. Ye, Y. Gogotsi, A.G. Yazicioglu, C.M. Megaridis, M. Yoshimura, Observation of water confined in nanometer channels of closed carbon nanotubes, Nano Lett. 4 (11) (2004) 2237–2243.
[10] J.K. Holt, H.G. Park, Y.M. Wang, M. Stadermann, A.B. Artyukhin, C.P. Grigoropulos, A. Noy, O. Bakajin, Fast mass transport through sub-2-nanometer carbon nanotubes, Science 312 (2006) 1034–1037.
[11] M. Majunder, N. Chopra, R. Andrews, B.J. Hinds, Nanoscale hydrodynamics: enhanced flow in carbon nanotubes, Nature 438 (2005) 44.
[12] G. Hummer, J.C. Rasaiah, J.P. Noworytra, Water conduction through the hydrophobic channel of a carbon nanotube, Nature 404 (2001) 188.
[13] P. Kumar, S.V. Buldyrev, Starr Francis F.W., N. Giovambattista, H.E. Stanley, Thermodynamics, structure, and dynamics of water confined between hydrophobic plates, Phys. Rev. E 72 (2005) 051503.
[14] J.R. Bordin, J.S. Soares, A. Diehl, M.C. Barbosa, Enhanced flow of core-softened fluids through narrow nanotubes, J. Chem. Phys. 140 (2014) 194504.
[15] M.H. Köhler, J.R. Bordin, L.B. da Silva, M.C. Barbosa, Breakdown of the Stokes–Einstein water transport through narrow hydrophobic nanotubes, Phys. Chem. Chem. Phys. 19 (2017) 12921–12927.
[16] J. Jin, L. Fu, H. Yang, J. Ouyang, Carbon hybridized halloysite nanotubes for high-performance hydrogen storage capacities, Scientific Reports 5 (2015) 12429.
[17] M.H. Köhler, R.C. Barbosa, L.B. da Silva, M.C. Barbosa, Role of the hydrophobic and hydrophilic sites in the dynamic crossover of the protein-hydration water, Phys. A 468 (2017) 733–739.
[18] Y. Xu, X. Tian, M. Lv, M. Deng, B. He, P. Xiu, Y. Tu, Y. Zheng, Effects of water-channel attractions on single-file water permeation through nanochannels, J. Phys. D: Appl. Phys. 49 (28) (2016) 285302.
[19] F. Ramazani, F. Ebrahimi, Uncertainties in the capillary filling of heterogeneous water nanochannels, J. Phys. Chem. C 120 (23) (2016) 12871–12878.
[20] J.R. Bordin, A.B. de Oliveira, A. Diehl, M.C. Barbosa, Diffusion enhancement in core-softened fluid confined in nanotubes, J. Chem. Phys 137 (2012) 084504.
[21] J.R. Bordin, M.C. Barbosa, Flow and structure of fluids in functionalized nanopores, Phys. A 467 (2017) 137–147.
[22] I. Moskowitz, M.A. Snyder, J. Mittal, Water transport through functionalized nanotubes with tunable hydrophobicity, J. Chem. Phys. 141 (2014) 18C532.
[23] S. Plimpton, Fast parallel algorithms for short-range molecular dynamics, J. Comput. Phys. 117 (1995) 1–19.
[24] J.L.F. Abascal, C. Vega, A general purpose model for the condensed phases of water: TIP4P/2005, J. Chem. Phys. 123 (2005) 234505.
[25] G. Raabe, R.J. Sadus, Molecular dynamics simulation of the effect of bond flexibility on the transport properties of water, J. Chem. Phys. 137 (2012) 104512.
[26] L. Liu, G.N. Patey, Simulated conduction rates of water through a (6,6) carbon nanotube strongly depend on bulk properties of the model employed, J. Chem. Phys. 144 (2016) 184502.
[27] K. Krynicki, C.D. Green, D.W. Sawyer, Pressure and temperature dependence of self-diffusion in water, Faraday Discuss. Chem. Soc. 66 (1978) 199–208.
[28] R.W. Hockney, J.W. Eastwood, Computer Simulation using Particles, McGraw-Hill, 1981.
[29] S. Nosé, A molecular dynamics method for simulation in the canonical ensemble, Mol. Phys. 52 (1984) 255.
[30] W.G. Hoover, Canonical dynamics: equilibrium phase-space distributions, Phys. Rev. A 31 (1985) 1695.
[31] J.P. Ryckaert, G. Ciccotti, H.J.C. Berendsen, Numerical integration of the cartesian equations of motion of a system with constraints: molecular dynamics of n-alkanes, J. Comput. Phys. 23 (1977) 327–341.
[32] P. Allen, D.J. Tildesley, Computer Simulation of Liquids, Oxford University Press, 1987.
[33] Y. Zheng, H. Ye, Z. Zhang, H. Zhang, Water diffusion inside carbon nanotubes: mutual effects of surface and confinement, Phys. Chem. Chem. Phys. 14 (2012) 964–971.
[34] M.H. Köhler, L.B. da Silva, Size effects and the role of density on the viscosity of water confined in carbon nanotubes, Chem. Phys. Lett. 645 (2016) 38–41.
[35] J.C. Rasaiah, S. Garde, G. Hummer, Water in nonpolar confinement: from nanotubes to proteins and beyond, Annu. Rev. Phys. Chem. 59 (2008) 713–740.
[36] S. Capponi, M. Heyden, A.-N. Bondar, D.J. Tobias, S.H. White, Anomalous behavior of water inside the secy translocon, Proc. Natl. Acad. Sci. USA 29 (2015) 9016–9021.
[37] K. Ritos, M.K. Borg, N.J. Mottram, J.M. Reese, Electric fields can control the transport of water in carbon nanotubes, Phil. Trans. R. Soc. A 374 (2016) 20150025.
[38] Winarto, D. Takaiwa, E. Yamamoto, K. Yasuoka, Structures of water molecules in carbon nanotubes under electric fields, J. Chem. Phys. 142 (2015) 124701.
[39] K. Koga, G.T. Gao, H. Tanaka, X.C. Zeng, Formation of ordered ice nanotubes inside carbon nanotubes, Nature 412 (2001) 802–805.
[40] Z.E. Hughes, C.J. Shearer, J. Shapter, J.D. Gale, Simulation of water transport through functionalized single-walled carbon nanotubes (swcnts), J. Phys. Chem. C 116 (2012) 24943–24953.
[41] G. Cicero, J.C. Grossman, E. Schwegler, F. Gygi, G. Galli, Water confined in nanotubes and between graphene sheets:a first principle study, J. Am. Chem. Soc. 130 (2008) 1871–1878.
[42] J.R. Bordin, A. Diehl, M.C. Barbosa, Relation between flow enhancement factor and structure for core-softened fluids inside nanotubes, J. Phys. Chem. B 117 (2013) 7047–7056.
[43] K. Zhao, H. Wu, Structure-dependent water transport across nanopores of carbon nanotubes: toward selective gating upon temperature regulation, Phys. Chem. Chem. Phys. 17 (2015) 10343–10347.
[44] Yu.D. Fomin, V.N. Ryzhov, E.N. Tsiok, The behaviour of water and sodium chloride solution confined into asbestos nanotube, Mol. Phys. 114 (15) (2016) 2279–2288.
[45] M. De Marzio, G. Camisasca, M.M. Conde, M. Rovere, P. Gallo, Structural properties and fragile to strong transition in confined water, J. Chem. Phys. 146 (8) (2017) 084505.
[46] R.J. Mash, S. Joseph, N.R. Aluru, Anomalously immobilized water: a new water phase induced by confinement in nanotubes, Nano Lett. 3 (2003) 589.
[47] A. Alexiadis, S. Kassinos, Molecular simulation of water in carbon nanotubes, Chem. Rev. 108 (2008) 5014.